Bioengineered 4:5, 332–337; September/October 2013; © 2013 Landes Bioscience

Analysis of gene expression on anodic porous alumina microarrays

Claudio Nicolini,[1,2,*] Manju Singh,[2] Rosanna Spera[2] and Lamberto Felli[3]

[1]Nanoworld Institute; Fondazione EL.B.A. Nicolini; Pradalunga, Italy; [2]Laboratories of Biophysics and Nanobiotechnology; Department of Experimental Medicine; University of Genova; Genova, Italy; [3]Department of Surgical Sciences and Integrated Diagnostic; University of Genova; Genova, Italy

Keywords: anodic porous alumina array, genes expression, NAPPA

This paper investigates the application of anodic porous alumina as an advancement on chip laboratory for gene expressions. The surface was prepared by a suitable electrolytic process to obtain a regular distribution of deep micrometric holes and printed by pen robot tips under standard conditions. The gene expression within the Nucleic Acid Programmable Protein Array (NAPPA) is realized in a confined environment of 16 spots, containing circular DNA plasmids expressed using rabbit reticulocyte lysate. Authors demonstrated the usefulness of APA in withholding the protein expression by detecting with a CCD microscope the photoluminescence signal emitted from the complex secondary antibody anchored to Cy3 and confined in the pores. Friction experiments proved the mechanical resistance under external stresses by the robot tip pens printing. So far, no attempts have been made to directly compare APA with any other surface/substrate; the rationale for pursuing APA as a potential surface coating is that it provides advantages over the simple functionalization of a glass slide, overcoming concerns about printing and its ability to generate viable arrays.

Introduction

Anodic porous alumina (APA) has attracted considerable attention because of its use as a template to manufacture nanostructures with a hexagonal arrangement of the nanopores as porous membranes,[1] nano ordered arrays[2] and nanoparticles[3] that have many applications in commercial electronic fields to detect biological molecules.[4,5] APA microarrays may be produced by a well-known two-step process involving anodic oxidation described by Masuda et al.[6] since distribution of highly ordered pores can hardly be achieved within a single-step method. The solid-state mechanisms of the formation of highly ordered pores in APA are complex and not yet completely understood. However, a few physical-chemical parameters, such as voltage, current density, electrolysis conditions and temperature, affect the final geometry of APA.

Recently there has been growing interest in the refinement of electrochemical techniques to optimize the APA preparation for possible applications in the biophysics field, such as diagnostics, enzymatic tests and other possible substrates applications to proteomics. In proteomics, different types of slides, such as glass or nylon, were used for gene expression or for the construction of an antibody microarray. Slides are commonly functionalized to anchor the antibody or the gene. APA allows the confinement of a biological sample in ordered pores. In particular, it has been used to spot Cy3-marked DNA and biological molecules.[7] Furthermore, APA has up to 10^4 per cm^2 where we can confine antibody or protein arrays to interact with other proteins.[8] Instead, the surface of glass slides for the deposition of protein is commonly functionalized by chemical or biological treatment. The purpose of this research is to find a method to amplify the dimension of the reduced hexagonal pores, as well as the number of pores in a square centimeter at the same time. We want to avoid the phenomena of capillarity—and we need to spot plasmid DNA on the surface of APA with antibody molecules—in order to study the expression of protein from genes and the interaction with alumina without altering the pore structure.

Results

Morphological analyses. The electrolytic process discussed above enables us to obtain hexagonal structures thare are 2–3 μm in diameter and have a density of pores of 2.7×10^{10} pores/cm^2, as shown in **Figure 1** by AFM topography. The analysis of the AFM profile allowed us to estimate the pore depth, which turned out to be approximately 700 nm. The much larger pore sizes allowed the plasmids to achieve their confinement in pores during the printing step.

Two tests were performed to characterize the mechanical properties of APA: a grip test and a ball-crush test, both performed in compliance with the DIN standards for mechanical evaluation (protocols DIN 4838 T 100, DIN 51097, DIN 51098 and DIN 51130). The grip test performed on APA over aluminum consists of measuring the mechanical force required to pull a pin (**Fig. 2A**), in contact with the analyzed surface forming an angle of 60°, across a linear path over the surface itself. The

*Correspondence to: Claudio Nicolini; Email: president@fondazioneelba-nicolini.org
Submitted: 03/06/13; Revised: 06/03/13; Accepted: 06/04/13
http://dx.doi.org/10.4161/bioe.25278

same test has been performed with two test pins with different tip diameters (10 and 60 microns). The drag path length was 15 mm, and exactly in the middle of the path, the surface changed from aluminum metal to APA. The increase of the friction is clearly visible, particularly for the thinner tip (this should be due to the more similar size of the tip and the APA pattern). This test proved that the grip of the APA surface has strongly increased with respect to the aluminum metal surface. The second test that was performed to mechanically characterize the APA surface was a ball-crush analysis,[10-12] which consisted of throwing small steel balls with controlled kinetic energy and impact angles ranging in 135° and then measuring the loss in weight of the blasted sample. The result of this experiment proved that about 60% of APA was pulverized by impacting steel balls. After these two tests, the main conclusion is that APA can grant a very good friction improvement (useful to attach it over any kind of compatible matter), but it isn't useful for direct mechanical stress (it must be handled with care).

The image of the CCD camera on the optical microscope operated at 100 × magnification reported in **Figure 2B** that pores are in agreement with the AFM results previously mentioned.[12] The number of pores on the APA surface is 1.4×10^7 with a mean distance of 3 μm. This average size of pores is larger than the normal size reported with common electrolyte reagents. In **Figure 2B**, we show the magnification of APA after the deposition of the plasmids. The surface on the left is uniformly flat with regularly distributed open pores, which appear as black circles with light walls. On the right, the CCD image—obtained after the printing of genes and of supporting biological material—shows the circumscribed spot circle to the square. With respect to the left image, collected at the same exposure intensity and acquisition time, the authors observed an irregular superimposed structure with a decreased density of open pores and an increased density of points reflecting light. The darker radial structures propagating from the edges of the spot toward the geometric center signal the interactions of the APA surface with the pen tip. The architecture of pores is maintained and was not destroyed by stresses induced by a robot, as suggested by the mechanical tests discussed above.

Electronic impedance spectrometry set up for NAPPA analysis. A possible solution to take advantage of the APA technology to host biomolecules in microarrays employs a label-free analysis as the electronic impedance spectrometry (EIS). It's well known that by using EIS, it is possible to detect different amounts of organic materials that are indirectly deposited over conducting surfaces. After the hybridization/expression experiment, using a scanning electrode controlled by a manipulator (MPC 200 by Sutter Technologies) via a PC, different EIS measurements were performed in different spots on the surface of the array using phosphate buffered saline solution (PBS); the walls of APA reduced the cross-talk effect so that the impedance parameters were measured almost exclusively as a function of the single spot over which the scanning electrode was placed when the single measurement was performed. In **Figure 2C**, it is possible to compare EIS plots traced when the scanning electrode was close (50 μm from the surface) to a test spot where the protein

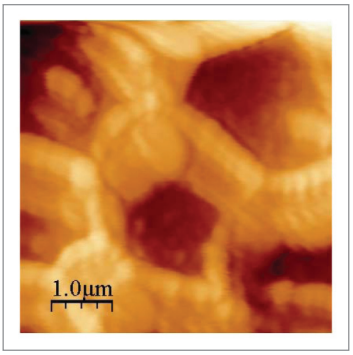

Figure 1. AFM image of a hexagonal order cell of APA.[9]

was expressed (straight line) and to another spot with the probe molecule only (dotted line). The two analysis spots were reciprocally only at a distance of 200 μm, and the experiments were performed using frequencies ranging from 1 Hz to 100 KHz, applying 400 mV peak to peak voltage.

Fluorescence measurements. The fluorescence signal of a sample depends on the concentration of Cy3 in the solution and the conformation of the protein on the surface of APA.[15] In particular, if the protein has a good degree of hydration and an optimal conformation, a large number of domains anchored to the exposed primary antibody can emit a fluorescence signal. Furthermore, we know from our experiments that the fluorescence signal from APA surface treated with Cy3 must be attributed to the complex linkage protein-antibody 1-antibody 2 with Cy3. Namely, the Cy3 fluorochrome unlinked to the complex was completely washed out from both holes and the pore walls, giving no fluorescence after three forced subsequent rinsing steps with Milli-Q water. The effects of a phosphate buffer, which were received in the expression kit and were preliminarily tested on APA, were as follows: the CCD images showed that the APA architecture is not affected by this treatment.

After the treatment with fluorochrome, circular spots with irregular shapes were detected on the APA surface as reported in **Figure 3A**. The traces of the robot pens are clearly shown in the concentric distribution (in particular in the right spot) and by the radii crossing the spots; correspondingly, the fluorescence signal of the protein expression is lower in these regions. We addressed these behaviors to the free arrangement of proteins in the growing process and their 3D folding, which influenced the pore structure as well as the geometry of the genes deposition by the robot. Furthermore, the spot enlarged in **Figure 3B** shows the fluorescence of a ring-like structure 800 μm apart from the main spot. A smaller ring is also observed close to the left spot. Conventional NAPPA on flat surfaces showed neither these side structures nor the fingerprint of the robot pen tip. At present, these findings in material as porous as APA point out the potential effects in the hydro-dynamical conditions between the solution drop from the robot pen and the hydrophobic nature of the APA surface.[16] In a flat surface, the solution deposited by the pen tip attains homogeneous distribution before water evaporation, cancelling the tip shape memory. In APA, the diffusion trend is prevented by pores, which confine the solution content within

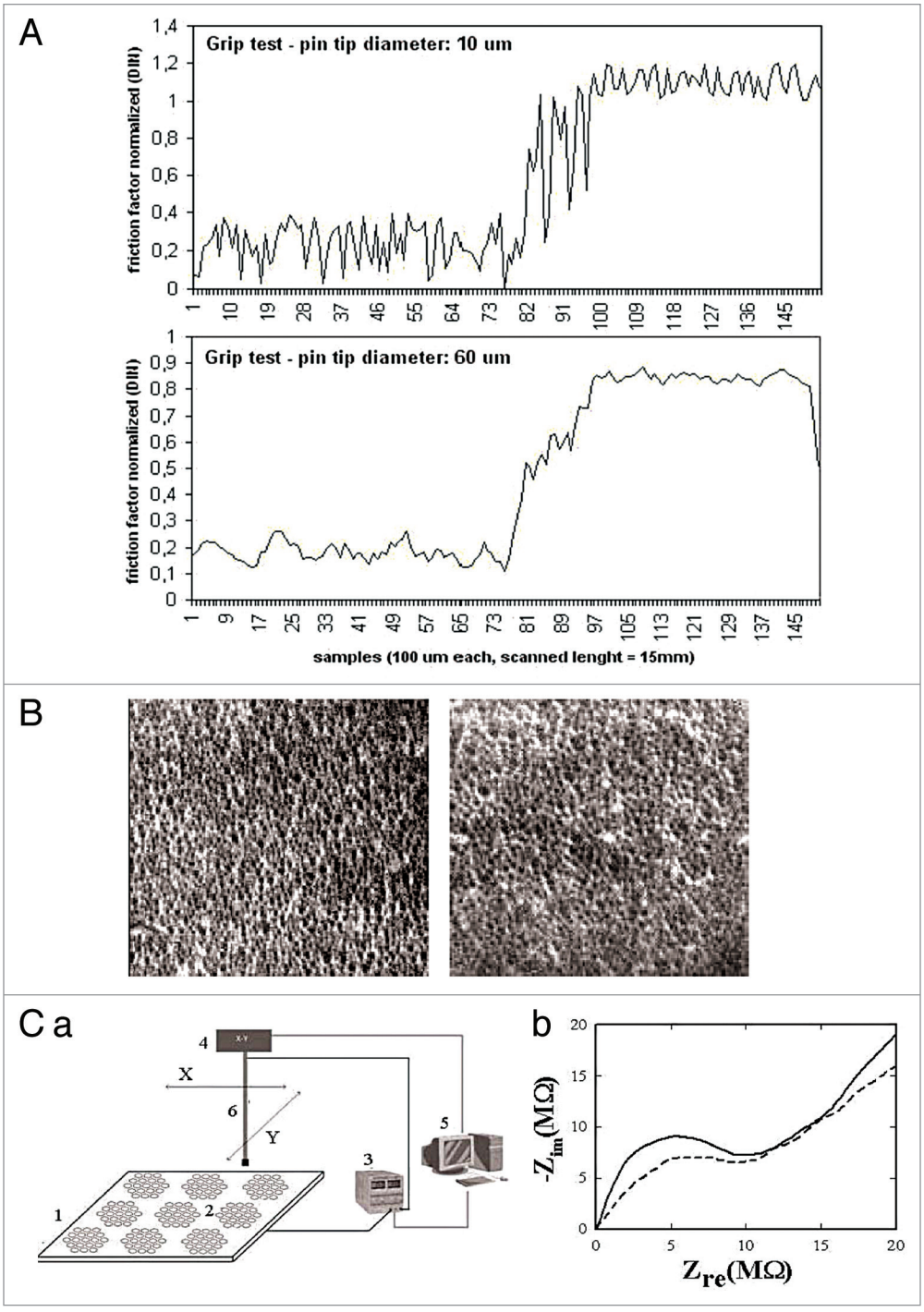

Figure 2. (**A**) Results of the friction test on the APA surface with pins of different sizes.[9,11] (**B**) CCD camera image of APA surface before (left) and after (right) printing. The full size of the square side is approximately 300 μm in both images. (**Ca**) Setup (instrumentation) to analyze NAPPA elements using impedentiometric measurements; 1, aluminum substrate, serving also as counter electrode; 2, APA spot, obtained by lithography, with bound biomolecules; 3, AC signal generator, controlled by PC; 4, XY bi-dimensional actuator, controlled by PC, positioning the scanning electrode upon spots; 5, PC, controlling bi-dimensional mover and AC signal generator; 6, Scanning electrode, dipped in the solution containing NAPPA and buffer. (b) Impedance spectroscopy behaviors in two spots of APA surface, the straight line with a protein hybridized to the probe molecule and the dotted line with probe only. Frequency ranges from 1 Hz to 100 KHz, voltage applied was 400 mVpp.[10,11]

pores. However, a minor fraction of the solution can exploit capillarity at APA edges between neighbor pores, and the hydrophobic character of APA can migrate away from the main spot, an effect that explains the many small spots observed around the main depositions. The two ring-like structures appear to be replicas of the two main spots, both for their shape and size and also for the pen fingerprint. These replicas are almost certainly a mechanical rebound due to the incomplete contact of the robot

pen with a porous surface. The combination of all these effects leads to the pattern observed in **Figure 3A and B**.

Discussion

We have proved the reliability of the APA surface in connection with the NAPPA technology, including its mechanical stability in the printing step. Furthermore, we proved the adaptability to chemical treatments, and to favor the protein expression within the same protocol, developed for more conventional substrates such as glass, mica, Teflon or nylon and gold. The favorable result suggests the prospect of confining the biological process, including genes and antibodies within a single pore, in the future and improving the present expression process toward smaller scales that can take place within a statistical distribution among many nearby pores. Additionally, APA significantly improves the fluorescence signal resolution that can be detected from single pores, achieving independent pore processes in arrays separated by a few microns with respect to the millimeter distances on glass or other flat surfaces, which is a necessity nowadays in biomedical applications. Present APA work with NAPPA aims to overcome the conflicting hydrodynamic conditions in addressing the printed gel solution at a micron scale. Statistical errors in false positive or false-negative results are indeed expected to drop significantly by exploiting both the improved fluorescence signal and the large number of available independent processes confined in pores.

Other possible biomedical applications. APA nanoporous materials have other numerous potential biological and medical applications that involve protein crystallography, sorting, sensing, isolating and releasing biological molecules. Nanoporous systems engineered to mimic natural filtration systems are actively being developed for use in smart implantable drug delivery systems, bioartificial organs and other novel nano-enabled medical devices. Moreover, the evolution of nanotechnology has provided new opportunities for using smaller and more regular structures for porous membranes. Artificial sieves with high precision and greater flexibility than track-etched membranes have been produced with improvements in performance and functionality;[17] these new filters have facilitated the most detailed scientific investigations of membrane-related phenomena to date. Many promising biomedical applications for nanoporous materials have recently been discovered, and several of these are currently being explored. Potential applications include use in implantable devices as well as in vitro analytical systems. In implantable drug delivery or immunoisolation devices, the membrane would function as a semipermeable compartment that holds the implant or drug while allowing passage of desired molecules in a controlled manner.[18] Nanoporous membranes are also the obvious choice for in vitro analysis, including medical diagnosis, cell evaluation and protein separation.[19] A key challenge has been to fabricate membranes with appropriate pore size, pore density and pore size distribution properties, in order to maximize passage of analytes and minimize passage of materials.[18,20,21] The pore diameter of nanoporous alumina membranes can also affect the behavior of hepatic cells.[22] The material itself showed no cytotoxic effects, and the cells adhered on the membranes even without any further surface modification. Cell proliferation increased with an increase in pore diameter and was highest on substrates with 200 nm pores. In contrast, cell functionality was nurtured on membranes with small pore diameters of around 50 nm. This suggests that it is possible to directly influence the response of HepG2 liver cells to the nanoporous substrates by varying the pore size of the membranes. The results highlight that nanometer surface features of a biomaterial are a key component during their interactions with biological tissues or cells. Recent progress in fabrication techniques has made it possible to make such ideal membranes inexpensively. The major difficulty in creating closed-loop systems that function over long periods of time within the body is the poor in vivo performance of implantable biosensors. Enormous research efforts in the past decade have been applied to automate biological analyses and to reduce sample consumption and cost. There has been a great push toward the microanalysis system (μTAS) or the lab-on-a-chip concept.[23]

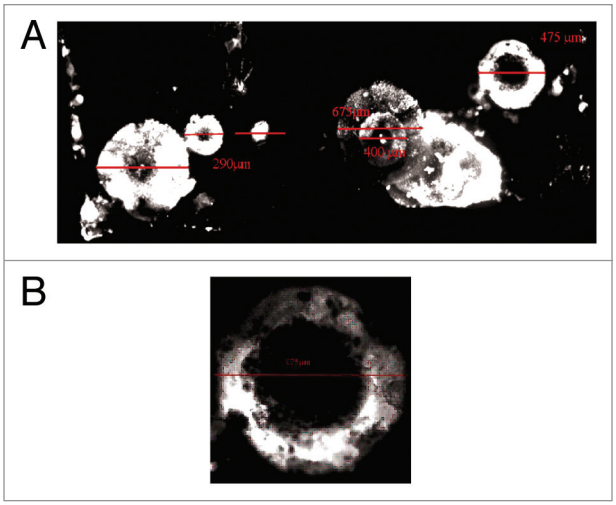

Figure 3. (**A**) Fluorescence image at the CCD camera after the protein expression protocol. Two main spots were printed by robot on this APA surface region, separated by 2 mm. The actual dimensions are reported on each fluorescence spot. (**B**) Enlargement of a ring-like growing distribution observed at a distance of 800 μm from the main spot.

Materials and Methods

We used Teflon for the construction of the laboratory-made electrochemical cell structure and pure grade platinum and 99.5% pure aluminum sheets 99.95% (Good Fellow) were used. Aluminum has not undergone further mechanical treatments of polishing by means of abrasive substances before use. Oxalic acid, sodium hydroxide, anhydride chromic, ethylene glycol and phosphoric acid were provided by Sigma Aldrich (Milan). All chemical reagents used in the series of experiments with analytical pure grade were used without further purification. The Promega kit contains parts of components necessary for the gene expression. Other components are contained in the kit Invitrogen. The mouse anti-FLAG M2 antibody was supplied from Sigma Aldrich. TNT R T7 coupled reticulocyte lysate system by Promega corporation was used for the phase of gene expression. The fluorochrome

Cy3 in concentration of 1 mg/ml was supplied by Amersham Biosciences. Milli-Q water with conductivity of 18 $m\Omega/cm^{-1}$ was supplied by Millipore Milli-Q system and used for rinsing phases. Anti-FLAG M2 antibodies (XYZ123 from Sigma) were also used. The sample genes were spotted by droplets on the APA surface by means of robot pens, which applies strength without causing surface damages. The gene expressions used were rabbit reticulocyte lysate, which have the complete ribosomal complex for the expression. After the expression, by Promega Kit (USA), we have obtained proteins with particular "orientation" onto the APA surface; Cy3 molecules have been linked to the sample proteins and fluorescence intensity has been assessed by CCD microscope. The results showed circular fluorescent areas for each spot of protein expressed. Keeping in mind that the most common commercial available pins are 300 μm diameter, the estimate deposition volume is 10 nl.[9-11]

Preparation of APA. We used 5 N high purity Al foils 0, 3 mm thickness as starting material for the electrolytic synthesis of APA (**Fig. 1**). The samples were cut by means of a microtome to avoid curvature effects of the surface that rises during the cutting phase of the Al piece to get a rectangular surface of 1 cm^2. Then, the sample was degreased in acetone for 5 min in ultrasonic vessel. The material was annealed into a stove at 420°C for 3 h onto a plain ceramic support, a step necessary to make the material tender for the following electrolysis phase. After 5 min sonication with ethanol to remove the surface roughness, Al was cleaned by electropolishing with a mixture of 69.5% perchloric acid and 99.5% ethanol with a ratio of 1:4 by using a Pt counter-electrode and applying a 20 V voltage for 3 min at 5°C into an ice bath. The apparatus used in this process is essentially an electrochemical cell made up by 2 electrodes placed vertically at a distance of 1.5 cm. After the electropolish phase, the material was thoroughly washed with Milli-Q water. Hence, the material underwent electrolysis for 30 min into a beaker of 500 ml containing a 0.3 M oxalic acid solution, keeping fixed the electrodes distance of 1.5 cm. Ethylene glycol was chosen as an inert additive during the anodization process and added to the solution at a concentration of 5.4 M to decrease the freezing point of the electrolyte. The electrolysis cooling system was fabricated by a serpentine with cryogenic fluids inside the beaker and an ice-salt mixture (cooling mixture) outside. After the first electrolysis, there is a rinsing step with a mixture of chromic anhydride (1.8 wt %) and phosphoric acid (5 wt %). This phase is necessary to remove the irregular layer of Al oxide formed during the previous step. The second phase of anodization lasts 1 h; at the end the substrate was washed with Milli-Q water to remove oxalic acid traces and sonicated for 20 min, then stored in a dry box before the AFM analysis and robot printing. The electric conductivity was measured to ascertain the achievement of an insulating oxide layer. The APA samples were sterilized in a vacuum stove at pressure of 1 atm and temperature of 140°C for three hours.

Biologic material deposition on the APA surface. The square-shaped substrate of APA platform with dimensions of 0.5 × 0.5 cm and manufactured with the procedure described above was anchored on a shaped piece of glass slide and processed at Harvard Institute of Proteomics (HIP) for genes[13] and antibodies printing.[9] Plasmid with the JUN gene inset and an antibody were anchored on the APA surface. The glutathione S-transferase (GST) tag present in the protein is required to bind the complementary sequence present in an antibody region. Near the plasmid an antibody is presented with complementary sequence to GST. Essentially, 10 μL of a solution of engineered DNA plasmid were deposited on APA surface by a robot; 16 spots were printed at a distance of 1 mm to each other. Water is quickly evaporated from the deposited droplets in the normal humidity conditions. In each spot, 400 plasmid genes were deposited. The samples were expressed following the Promega Kit protocol.

AFM and CCD camera microscope. An atomic force microscopy (SPMagic by Elbatech srl, Italy) was employed to characterize the morphology of APA surface.[12] The images of the samples were elaborated with freeware WSxM 4.0 software[14] particularly to evaluate both mean pore sizes and the mean pore depth. Images were obtained in tapping mode by using a standard SNC-18 tip. Fluorescence of the sample was collected by using a CCD camera equipped with model software for compute the intensity of fluorochrome Cy3. The CCD microscope was presented a module that contains a mercury lamp that uses filters to select 530 nm of fluorescence signal. The images (**Fig. 2B**) are acquired with the software Axio Vision 3.1. In live mode the images are recorded with a fixed exposition time of 187 ms and 10× magnification in a dark room. The luminosity intensity of the images was normalized by a factor of two to avoid saturation. Cy3 has the capability to emit photons with a shorter wavelength in a period of 10^{-9}–10^{-8} s after 530 nm green light excitation (absorption). A red filter was adopted to obtain a pure fluorescence signal image.

Disclosure of Potential Conflicts of Interest

No potential conflict of interest was disclosed.

Acknowledgments

This project was supported by MIUR (Ministero dell'Istruzione, Università e Ricerca) to Fondazione Elba Nicolini with annual grants for "Funzionamento" and to CN at the University of Genova for FIRB Italnanoitalnet RBPR05JH2P_04. We are particularly gratefull to Stura I and Larosa I for their contributions during their PhD thesis here quoted.

References

1. Xu XJ, Fei GT, Zhu LQ, Wang XW. A facile approach to the formation of the alumina nanostructures from anodic alumina membranes. Mater Lett 2006; 60:2331-4; http://dx.doi.org/10.1016/j.matlet.2006.01.001
2. Hobbs KL, Larson PR, Lain GD, Keay JC, Johnson MB. Fabrication of nanoring arrays by sputter redeposition using porous alumina templates. Nano Lett 2004; 4:167-71; http://dx.doi.org/10.1021/nl034835u
3. Xei G, Song M, Mitsuishi K, Furuya K. Characterization of metal nanoparticles fabricated in ordered array pores of anodic porous alumina by electron-beam-induced selective deposition. Appl Surf Sci 2005; 241:91-5; http://dx.doi.org/10.1016/j.apsusc.2004.09.023
4. Stura E, Bruzzese D, Valerio F, Grasso V, Perlo P, Nicolini C. Anodic porous alumina as mechanical stability enhancer for LDL-cholesterol sensitive electrodes. Biosens Bioelectron 2007; 23:655-60; PMID:17766101; http://dx.doi.org/10.1016/j.bios.2007.07.011
5. Nicolini C, LaBaer J. Nanotechnology applications of Nucleic Acid Programmable Protein Arrays, in Functional Proteomics and Nanotechnology-based Microarrays, Vol. 2 (Nicolini C, LaBaer J, Eds.). Pan Stanford Series on Nanobiotechnology, London - New York - Singapore, 2010, Ch. 1.
6. Masuda H, Fukuda K. Ordered metal nanohole arrays made by a two-step replication of honeycomb structures of anodic alumina. Science 1995; 268:1466-8; PMID:17843666; http://dx.doi.org/10.1126/science.268.5216.1466
7. Matsumoto F, Nishio K, Masuda H. Flow-Through-Type DNA Array Based on Ideally Ordered Anodic Porous Alumina Substrate. Advanced Materials 2004; 16:2102-5; http://dx.doi.org/10.1002/adma.200400360
8. Grasso V, Lambertini VV, Ghibellini P, Valerio F, Stura E, Perlo P, et al. Nanostructuring of a porous alumina matrix for a biomolecular microarray. Nanotechnology 2006; 17:795-8; http://dx.doi.org/10.1088/0957-4484/17/3/030
9. Stura E, Larosa C, Bezerra Correia Terencio T, Hainsworth E, Ramachandran N, LaBaer J, et al. Label-free NAPPA: Anodic Porous Alumina, in Functional Proteomics and Nanotechnology-based Microarrays (Nicolini C, LaBaer J, Eds.). Pan Stanford Series on Nanobiotechnology Volume 2, Chapter 5, pp. 95-108, London - New York - Singapore, 2010.
10. Nicolini C, Bragazzi N, Pechkova E. Nanoproteomics enabling personalized nanomedicine. Adv Drug Deliv Rev 2012; 64:1522-31; PMID:22820526; http://dx.doi.org/10.1016/j.addr.2012.06.015
11. Nicolini C, Bezerra Correia T, Stura E, Larosa C, Spera C, Pechkova E. Atomic Force Microscopy And Anodic Porous Allumina Of Nucleic Acid Programmable Protein Arrays. BIOT 2012.
12. Moadhen A, Elhouichet H, Nosova L, Oueslati M, Rhodamine B. Absorbed by anodic porous alumina: Stokes and anti-Stokes luminescence study. J Lumin 2007; 126:789-94; http://dx.doi.org/10.1016/j.jlumin.2006.11.013
13. Redón R, Vázquez-Olmos A, Mata-Zamora ME, Ordóñez-Medrano A, Rivera-Torres F, Saniger JM. Contact angle studies on anodic porous alumina. J Colloid Interface Sci 2005; 287:664-70; PMID:15925635; http://dx.doi.org/10.1016/j.jcis.2005.02.036
14. Han JY, Fu JP, Schoch RB. Molecular sieving using nanofilters: past, present and future. Lab Chip 2008; 8:23-33; PMID:18094759; http://dx.doi.org/10.1039/b714128a
15. Leoni L, Boiarski A, Desai TA. Characterization of Nanoporous Membranes for Immunoisolation: diffusion properties and tissue effects. Biomedical Microdevices 2002; 4:131-9; http://dx.doi.org/10.1023/A:1014639332543.
16. Gatimu EN, Sweedler JV, Bohn PW. Nanofluidics and the role of nanocapillary array membranes in mass-limited chemical analysis. Analyst 2006; 131:705-9; PMID:16732357; http://dx.doi.org/10.1039/b600158k
17. Huang Z. Nanoporous Alumina Membrane for Enhancing Hemodialysis. Journal of Medical Devices. 2007; 1:79-83; http://dx.doi.org/10.1115/1.2360949
18. Martin F, Walczak R, Boiarski A, Cohen M, West T, Cosentino C, et al. Tailoring width of microfabricated nanochannels to solute size can be used to control diffusion kinetics. J Control Release 2005; 102:123-33; PMID:15653139; http://dx.doi.org/10.1016/j.jconrel.2004.09.024
19. Hoess A, Thormann A, Friedmann A, Heilmann A. Self-supporting nanoporous alumina membranes as substrates for hepatic cell cultures. J Biomed Mater Res A 2012; 100:2230-8; PMID:22492687
20. Han J. In: Di Ventra M, Evoy S, Heflin JR (ed). Introduction to Nanoscale Science and Technology. Springer, New York 2004.
21. Ramachandran N, Raphael JV, Hainsworth E, Demirkan G, Fuentes MG, Rolfs A, et al. Next-generation high-density self-assembling functional protein arrays. Nat Methods 2008; 5:535-8; PMID:18469824; http://dx.doi.org/10.1038/nmeth.1210
22. Racapé M, Bragazzi N, Sivozhelezov V, Danger R, Pechkova E, Duong Van Huyen JP, et al. SMILE silencing and PMA activation gene networks in HeLa cells: comparison with kidney transplantation gene networks. J Cell Biochem 2012; 113:1820-32; PMID:22134986; http://dx.doi.org/10.1002/jcb.24013
23. Horcas I, Fernández R, Gómez-Rodríguez JM, Colchero J, Gómez-Herrero J, Baro AM. WSXM: a software for scanning probe microscopy and a tool for nanotechnology. Rev Sci Instrum 2007; 78:013705; PMID:17503926; http://dx.doi.org/10.1063/1.2432410